

The Low-volatility Anomaly and the Adaptive Multi-Factor Model*

Robert A. Jarrow[†], Rinald Murataj[‡], Martin T. Wells[§], Liao Zhu[¶]

Abstract

The paper provides a new explanation of the low-volatility anomaly. We use the Adaptive Multi-Factor (AMF) model estimated by the Groupwise Interpretable Basis Selection (GIBS) algorithm to find those basis assets significantly related to low and high volatility portfolios. These two portfolios load on very different factors, indicating that volatility is not an independent risk, but that it's related to existing risk factors. The out-performance of the low-volatility portfolio is due to the (equilibrium) performance of these loaded risk factors. The AMF model outperforms the Fama-French 5-factor model both in-sample and out-of-sample.

Keywords: Low-volatility anomaly, AMF model, GIBS algorithm, high-dimensional statistics, machine learning, False Discovery Rate.

JEL: C10 (Econometric and Statistical Methods and Methodology: General), G10 (General Financial Markets: General)

*We thank Dr. Manny Dong, and all the support from Cornell University. The author names are in alphabetical order. Disclaimer: All opinions and inferences are attributable to the authors and do not represent the views of the T. Rowe Price Associates, Inc.

[†]Ronald P. and Susan E. Lynch Professor of Investment Management, Samuel Curtis Johnson Graduate School of Management, Cornell University, Ithaca, New York 14853, USA and Kamakura Corporation, Honolulu, Hawaii 96815. Email: raj15@cornell.edu.

[‡]Quantitative Analyst at T. Rowe Price, Baltimore, Maryland. Email: rinald.murataj@troweprice.com

[§]Charles A. Alexander Professor of Statistical Sciences, Department of Statistics and Data Science, Cornell University, Ithaca, New York 14853, USA. Email: mtw1@cornell.edu.

[¶]Ph.D. in the Department of Statistics and Data Science, Cornell University, Ithaca, New York 14853, USA. Email: lz384@cornell.edu.

1 Introduction

The low-risk anomaly is the empirical observation that stocks with lower risk yield higher returns than stocks with higher risk. Here risk is quantified as either a security’s return volatility or a security’s beta as derived from a Capital Asset Pricing Model (CAPM). This paper focuses only on the low-volatility anomaly.¹ The low-risk anomaly contradicts accepted APT or CAPM theories that higher risk portfolios earn higher returns. The low-risk anomaly is not a recent empirical finding but an observation documented by a large body of literature dating back to the 1970s. A brief review of the low-risk anomaly literature can be found in appendix A. Despite its longevity, the academic community differs over the causes of the anomaly. The two main explanations are: 1) it is due to leverage constraints that retail, pension, and mutual fund investors face which limits their ability to generate higher returns by owning lower risk stocks, and 2) it is due to behavioral biases including the lottery demand for high beta stocks, institutions beating index benchmarks with limits to arbitrage, and sell-side analysts over-bias on high volatility stock earnings.

This paper provides a new explanation for the low-volatility anomaly using the newly developed high-dimensional methods based Groupwise Interpretable Basis Selection (GIBS) algorithm with the Adaptive Multi-Factor (AMF) model as [Zhu et al. \(2020\)](#).

The new insights are due to the advantages of the GIBS algorithm when estimating the AMF model in contrast to the existing methods. The existing methods trace back to the original papers by [Ross \(1976\)](#) Arbitrage Pricing Theory (APT) and [Merton \(1973\)](#) Inter-temporal Capital Asset Pricing Model (ICAPM), updated with the recent insights of [Feng et al. \(2017\)](#), [Kozak et al. \(2018\)](#), [Giglio and Xiu \(2019\)](#), and [Giglio et al. \(2020\)](#). These recent papers typically either add factors one-by-one using some refined significance testing procedures, or they use Principal Component Analysis (PCA) or variance-decomposition methods to find a small number of factors. The PCA either mixes the underlying risk-factors or separates them into several principal components, both of which cause interpretation problems. The sparse PCA method used in [Kozak et al. \(2018\)](#) removes some of the weaknesses of the traditional PCA, and even gives an

¹In analyzing the low-beta anomaly, an issue is the non synchronized trading of small stocks, where a small stock may trade less frequently than the index it is regressed on (market return) to obtain the stock’s beta (see [McInish and Wood \(1986\)](#)).

interpretation of the risk-factors as stochastic discount risk-factors. However, all these methods still suffer from the problems (low interpretability, low prediction accuracy, etc.) inherited from the variance decomposition framework.

The GIBS algorithm changed this framework in the following ways. First, it abandons the variance decomposition framework and is not based on PCA. Instead, it is based on the prototype clustering and high-dimensional methods. It selects basis assets as the “prototypes” or “center” of the groups they are representing, which gives a clearer interpretation and improved prediction accuracy. Second, instead of searching for a few common risk-factors that affect the entire cross-section of expected returns as in the conventional approach, the GIBS algorithm also finds groupwise basis assets which may only affect stocks in a specific group, sector, or industry. These advantages provide new insights into the low-volatility anomaly.

The GIBS algorithm was developed to estimate the Adaptive Multi-Factor (AMF) model (see [Zhu et al. \(2020\)](#)) which includes both the APT and ICAPM as special cases. The AMF is derived under a weaker set of assumptions using the recently developed Generalized Arbitrage Pricing Theory ([Jarrow and Protter \(2016\)](#)). Its time-invariance is tested in [Zhu et al. \(2021\)](#). Its three main benefits are: 1) it is consistent with a large number of risk factors being needed to explain all security returns, 2) yet, the set of risk factors is small for any single security and different for different securities, and 3) the risk factors are traded. These benefits imply that the underlying model estimated is more robust than those used in the existing literature. In [Zhu et al. \(2020\)](#), basis assets (formed from the collection of Exchange Traded Funds (ETF)) are used to capture risk factors in *realized* returns across securities. Since the collection of basis assets is large and highly correlated, high-dimension methods (including the LASSO and prototype clustering) are used. This paper employs the same methodology to investigate the low-volatility anomaly. We find that high-volatility and low-volatility portfolios load on different basis assets, which indicates that volatility is not an independent risk. The out-performance of the low-volatility portfolio is due to the (equilibrium) performance of these loaded risk factors. For completeness, we compare the AMF model with the traditional Fama-French 5-factor (FF5) model, documenting the superior performance of the AMF model.

An outline for this paper is as follows. Section 2 discusses the estimation methodology, and section 3 presents the results. Section 4 concludes. A brief review of the high

dimensional statistical methods used in this paper is in Appendix B.

2 The Estimation Methodology

This section gives the estimation methodology. We first pick the universe of stocks and ETFs, so that we only focus on the assets that are easy to trade. Then, we form the high and low volatility portfolios and we choose a time period that exhibits the low-volatility anomaly. We will employ the Adaptive Multi-Factor (AMF) asset pricing model with the Groupwise Interpretable Basis Selection (GIBS) algorithm to these two portfolios and analyze the results in a subsequent section.

2.1 The Stock and ETF Universe

The data initially consists of all stocks and ETFs available in the Center for Research in Security Prices (CRSP) database. To ensure all our securities are actively traded, we focus on stocks and ETFs with a market capitalization ranking in top 2500. This filter excludes small stocks that are more likely to exhibit the low-volatility anomaly. In addition, we select stocks and ETFs satisfying the following criteria.

1. According to the description of the CRSP database, ETFs should be with a Share Code (SHRCD) 73. We follow this common practice.
2. We excluded American Depositary Receipts (ADR) from our stock universe. Removing the ADR is a common practice in all empirical finance papers and the main reason is that they are not part of the indices. This is achieved by using the Share Code (SHRCD) 10 or 11 from the CRSP dataset.
3. We only choose ETFs and stocks which are listed on the NYSE, AMEX and NASDAQ exchanges. This is obtained with the Exchange Code (EXCHCD) 1, 2 or 3 from the CRSP dataset.
4. For a stock to be included at time t , its return has to be observable at least 80% of trading times in the previous year in order to calculate its volatility. For an ETF to be considered at time t , its return has to be observable during the 3-year regression window before time t .

The number of ETFs in our universe increased rapidly after 2003, see Figure 1. To apply the AMF model and GIBS algorithm, we need enough ETFs to form our collection of basis assets. Hence, we begin our analysis in 2003. To understand the dimension of the set of basis assets, we calculate both the GIBS dimension and the Principal Component Analysis (PCA) dimension of the ETFs in our universe. The PCA dimension at time t is defined to be the number of principal components needed to explain 90% of the variance during the previous 3-years. The GIBS dimension is defined to be the number of “representatives” selected using the GIBS algorithm from the basis assets, i.e. the cardinality of the set U in Table 1. The GIBS and PCA dimensions of the ETFs across time are shown in Figure 2.

Comparing Figures 1 and 2, we see that the number of ETFs and dimensions increase over this time period. The GIBS and PCA dimension do not increase as fast as the number of ETFs. But, the GIBS dimension increases faster than the PCA dimension, suggesting that GIBS is able to pick more basis assets than does the PCA. The reason is that PCA mixes basis assets together in linear combinations, while the GIBS algorithm does not.

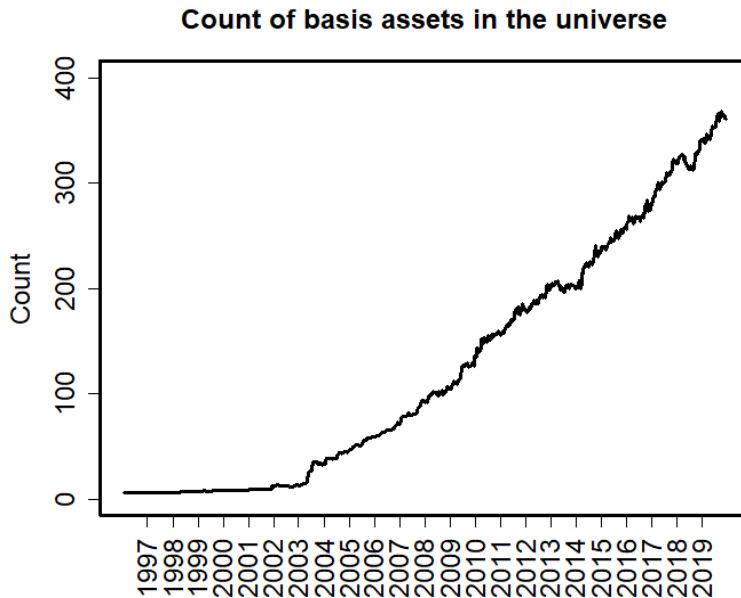


Figure 1: Count of the ETFs in the universe.

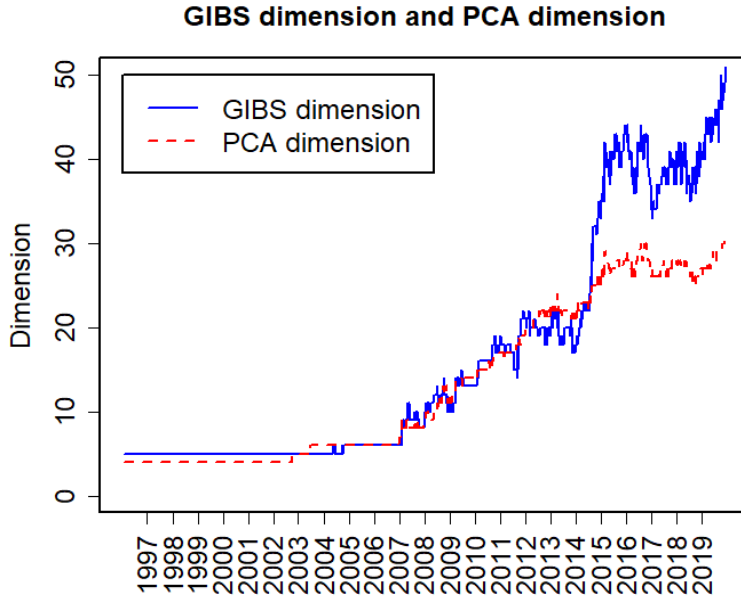


Figure 2: GIBS dimension and PCA dimension of ETFs in the universe.

2.2 Portfolios and the Low-volatility Anomaly

To study the low-volatility anomaly, we need to form the high- and low-volatility portfolios. To do this, we first calculate the volatility of the stocks in our universe at time t as the standard deviation of their excess returns over the previous year. The excess return is the raw return minus the risk free rate. Using the excess return is a common practice in the empirical finance literature since it removes the risk free rate and focuses on the risk premiums. The high-volatility portfolio is constructed as an equal-weighted portfolio using the stocks with the highest 25% volatilities. Similarly, we take the stocks having the lowest 25% volatilities to form the low-volatility portfolio. To avoid a survivorship bias, we include the delisted returns (see [Shumway \(1997\)](#) for more explanation).

We then compare the excess returns of the high- and low-volatility portfolios to verify the existence of the low-volatility anomaly over our sample period. Given the graph, we selected 2008 as the start of the anomaly. Between 2008 - 2018, the low-volatility portfolio had an excess return of 121.4%, which is higher than the 62.5% excess return of the high-volatility portfolio. This documents the existence of the low-volatility anomaly over

our sample period. The superior performance of the low-volatility portfolio is manifested in Figure 3 which graphs the cumulative value of the two portfolios starting from \$1 at the beginning of 2008.

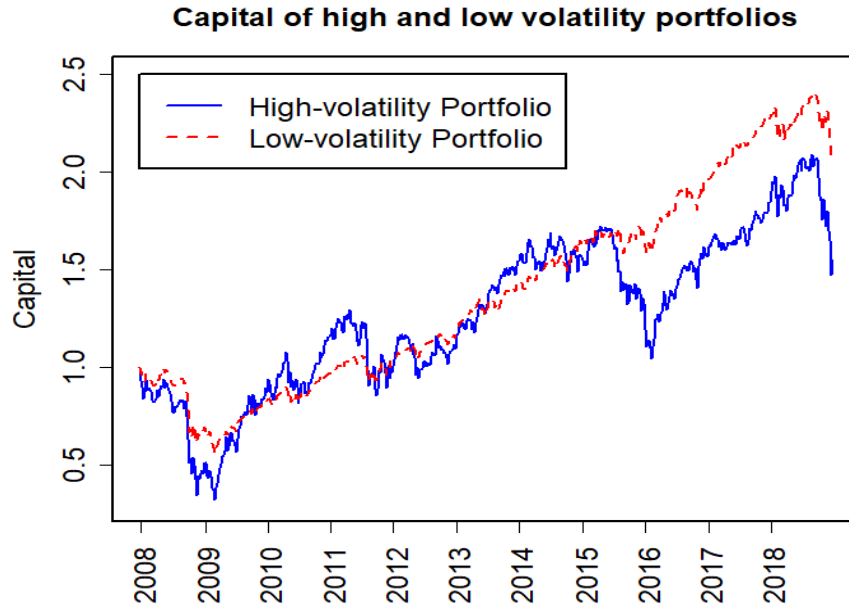


Figure 3: Cumulative value of the excess returns from the high- and low-volatility portfolios.

2.3 The AMF and GIBS Estimation

This section estimates the Adaptive Multi-Factor (AMF) model based on the Groupwise Interpretable Basis Selection (GIBS) algorithm proposed by [Zhu et al. \(2020\)](#). Although a brief review of the AMF model and the GIBS algorithm are included in this section, the details can be found in [Zhu et al. \(2020\)](#). A sketch of the GIBS algorithm is in Table 1 at the end of this section.

To avoid the effects of market micro-structure frictions, we use a weekly horizon. Because the number of ETFs increase over time and the market structure changes during the financial crisis, to approximate stationarity, we pick a 3-year regression window to do the analysis. In addition, because the number of ETFs exceed the number of observations

within each regression window, we are in the high-dimensional regime. Therefore, the high-dimensional GIBS algorithm needs to be used to estimate the AMF model. We use a dynamic version of the GIBS algorithm applied to rolling windows. For each week t in 2008 - 2018, we use the time period from 3 years (156 weeks) window earlier as our current regression window. We use all the ETFs in our universe as described in Section 2.1 and the FF5 factors as our basis assets. Then, we apply the GIBS algorithm to select the GIBS determined basis assets and use them to explain the excess returns of the high- and low-volatility portfolios using the AMF model. The following is a more detailed introduction to the AMF model and the GIBS algorithm within each time window.

In the asset pricing theory, given a frictionless, competitive, and arbitrage free market, a dynamic generalization of Ross (1976) APT and Merton (1973) ICAPM is contained in Jarrow and Protter (2016). This extension implies that the Adaptive Multi-Factor (AMF) model holds for any security's return over $[t, t + 1]$:

$$R_i(t) - r_0(t) = \sum_{j=1}^p \beta_{i,j} [r_j(t) - r_0(t)] = \boldsymbol{\beta}'_i \cdot [\mathbf{r}(t) - r_0(t)\mathbb{1}] \quad (1)$$

where $R_i(t)$ denotes the return of the i -th security for $1 \leq i \leq N$ (where N is the number of securities), $r_j(t)$ denotes the return on the j -th basis asset for $1 \leq j \leq p$, $r_0(t)$ is the risk free rate, $\mathbf{r}(t) = (r_1(t), r_2(t), \dots, r_p(t))'$ denotes the vector of security returns, $\mathbb{1}$ is a column vector with every element equal to one, and $\boldsymbol{\beta}_i = (\beta_{i,1}, \beta_{i,2}, \dots, \beta_{i,p})'$.

In this paper we are only concerned with the low- and high-volatility portfolios. Let R_1 denote the raw return of the low-volatility portfolio and R_2 the raw return of the high-volatility portfolio. To empirically test our model, both an intercept α_i and a noise term $\epsilon_i(t)$ are added to expression (1), i.e.

$$R_i(t) - r_0(t) = \alpha_i + \sum_{j=1}^p \beta_{i,j}(t) [r_j(t) - r_0(t)] + \epsilon_i(t) = \alpha + \boldsymbol{\beta}'_i [\mathbf{r}(t) - r_0(t)\mathbb{1}] + \epsilon_i(t) \quad (2)$$

where $\epsilon_i(t) \stackrel{iid}{\sim} N(0, \sigma_i^2)$ and $1 \leq i \leq N$. The intercept enables the testing for mispriced securities, and the error term allows for noise in the return observations.

As mentioned earlier, using weekly returns over a 3-year time period necessitates the use of high-dimensional statistics. To understand why, consider the following. For a given

time period (t, T) , letting $n = T - t + 1$, we can rewrite expression (2) as

$$\mathbf{R}_i - \mathbf{r}_0 = \alpha_i \mathbb{1}_n + (\mathbf{r} - \mathbf{r}_0 \mathbb{1}'_p) \boldsymbol{\beta}_i + \boldsymbol{\epsilon}_i \quad (3)$$

where $1 \leq i \leq N$, $\boldsymbol{\epsilon}_i \sim N(0, \sigma_i^2 \mathbf{I}_n)$ and

$$\begin{aligned} \mathbf{R}_i &= \begin{pmatrix} R_i(t) \\ R_i(t+1) \\ \vdots \\ R_i(T) \end{pmatrix}_{n \times 1}, \quad \mathbf{r}_0 = \begin{pmatrix} r_0(t) \\ r_0(t+1) \\ \vdots \\ r_0(T) \end{pmatrix}_{n \times 1}, \quad \boldsymbol{\epsilon}_i = \begin{pmatrix} \epsilon_i(t) \\ \epsilon_i(t+1) \\ \vdots \\ \epsilon_i(T) \end{pmatrix}_{n \times 1} \\ \boldsymbol{\beta}_i &= \begin{pmatrix} \beta_{i,1} \\ \beta_{i,2} \\ \vdots \\ \beta_{i,p} \end{pmatrix}_{p \times 1}, \quad \mathbf{r}_i = \begin{pmatrix} r_i(t) \\ r_i(t+1) \\ \vdots \\ r_i(T) \end{pmatrix}_{n \times 1}, \quad \mathbf{r}(t) = \begin{pmatrix} r_1(t) \\ r_2(t) \\ \vdots \\ r_p(t) \end{pmatrix}_{p \times 1} \\ \mathbf{r}_{n \times p} &= (\mathbf{r}_1, \mathbf{r}_2, \dots, \mathbf{r}_p)_{n \times p} = \begin{pmatrix} \mathbf{r}(t)' \\ \mathbf{r}(t+1)' \\ \vdots \\ \mathbf{r}(T)' \end{pmatrix}_{n \times p}, \quad \mathbf{R} = (\mathbf{R}_1, \mathbf{R}_2, \dots, \mathbf{R}_N) \end{aligned} \quad (4)$$

Recall that the coefficients β_{ij} are assumed to be constants. This assumption is only reasonable when the time period (t, T) is small (say 3 years), so the number of observations is $n \approx 150$. However, the number of basis assets p , is around 300 in recent years, implying that the independent variables exceed the observations.

Because of this high-dimension problem and the high-correlation among the basis assets, traditional methods fail to give an interpretable and systematic way to fit the Adaptive Multi-Factor (AMF) model. Therefore, we employ the Groupwise Interpretable Basis Selection (GIBS) algorithm to select the basis assets set $S \subseteq \{1, 2, \dots, p\}$ (the derivation of S is provided later). Then, the model becomes

$$\mathbf{R}_i - \mathbf{r}_0 = \alpha_i \mathbb{1}_n + (\mathbf{r}_S - (\mathbf{r}_0)_S \mathbb{1}'_p) (\boldsymbol{\beta}_i)_S + \boldsymbol{\epsilon}_i. \quad (5)$$

The notation \mathbf{r}_S denotes the columns in the matrix $\mathbf{r}_{n \times p}$ indexed by the index set

$S \subseteq \{1, 2, \dots, p\}$, and $(\mathbf{r}_0)_S$ denotes the elements in the vector $(\mathbf{r}_0)_{n \times 1}$ indexed by the index set $S \subseteq \{1, 2, \dots, p\}$. We will use this notation for any matrices, vectors and indices sets throughout this paper. An example of expression (5) is the [Fama and French \(2015\)](#) 5-factor (FF5) model where all of the basis assets are risk-factors, earning non-zero expected excess returns. However, FF5 assumes that the number of risk-factors is small and common to all the securities, whereas the AMF and GIBS does not.

Next, we give a brief review of the GIBS algorithm. For notation simplicity, denote

$$\mathbf{Y}_i = \mathbf{R}_i - \mathbf{r}_0, \quad \mathbf{X}_i = \mathbf{r}_i - \mathbf{r}_0, \quad \mathbf{Y} = \mathbf{R} - \mathbf{r}_0, \quad \mathbf{X} = \mathbf{r} - \mathbf{r}_0 \quad (6)$$

where the definitions of \mathbf{R}_i , \mathbf{R} , \mathbf{r}_i , \mathbf{r} are in equations (3 - 4). Let \mathbf{r}_1 denote the market return. It is easy to check that most of the ETF basis assets \mathbf{X}_i are correlated with \mathbf{X}_1 (the market return minus the risk free rate). We note that this pattern is not true for the other four Fama-French factors. Therefore, we first orthogonalize every other basis asset to \mathbf{X}_1 . By orthogonalizing with respect to the market return, we avoid choosing redundant basis assets similar to it and also increase the accuracy of fitting. Note that for the Ordinary Least-Square (OLS) regression, projection does not affect the estimation since it only affects the coefficients, not the estimated $\hat{\mathbf{y}}$. However, in high-dimension methods such as LASSO, projection does affect the set of selected basis assets because it changes the magnitude of shrinking. Thus, we compute

$$\widetilde{\mathbf{X}}_i = (\mathbf{I} - P_{\mathbf{X}_1})\mathbf{X}_i = (\mathbf{I} - \mathbf{X}_1(\mathbf{X}'_1\mathbf{X}_1)^{-1}\mathbf{X}'_1)\mathbf{X}_i \quad \text{where } 2 \leq i \leq p_1 \quad (7)$$

where $P_{\mathbf{X}_1}$ denotes the projection operator, and p_1 is the number of columns in $\mathbf{X}_{n \times p_1}$. Denote the vector

$$\widetilde{\mathbf{X}} = (\mathbf{X}_1, \widetilde{\mathbf{X}}_2, \widetilde{\mathbf{X}}_3, \dots, \widetilde{\mathbf{X}}_{p_1}). \quad (8)$$

Note that this is equivalent to the residuals after regressing other basis assets on the market return minus the risk free rate.

The transformed ETF basis assets $\widetilde{\mathbf{X}}$ still contain highly correlated members. We first divide these basis assets into categories A_1, A_2, \dots, A_k based on a financial characterization. Note that $A \equiv \cup_{i=1}^k A_i = \{1, 2, \dots, p_1\}$. The list of categories with more descriptions can be found in [Appendix D](#). The categories are (1) bond/fixed income, (2) commodity,

(3) currency, (4) diversified portfolio, (5) equity, (6) alternative ETFs, (7) inverse, (8) leveraged, (9) real estate, and (10) volatility.

Next, from each category we need to choose a set of representatives. These representatives should span the categories they are from, but also have low correlation with each other. This can be done by using the prototype-clustering method with a distance measure defined by equation (20), which yield the “prototypes” (representatives) within each cluster (intuitively, the prototype is at the center of each cluster) with low-correlations.

Within each category, we use the prototype clustering methods previously discussed to find the set of representatives. The number of representatives in each category can be chosen according to a correlation threshold. This gives the sets B_1, B_2, \dots, B_k with $B_i \subset A_i$ for $1 \leq i \leq k$. Denote $B \equiv \cup_{i=1}^k B_i$. Although this reduction procedure guarantees low-correlation between the elements in each B_i , it does not guarantee low-correlation across the elements in the union B . So, an additional step is needed, in which prototype clustering on B is used to find a low-correlated representatives set U . Note that $U \subseteq B$. Denote $p_2 \equiv \#U$.

Recall from the notation definition in equation (12) that $\widetilde{\mathbf{X}}_U$ means the columns of the matrix $\widetilde{\mathbf{X}}$ indexed by the set U . Since basis assets in $\widetilde{\mathbf{X}}_U$ are not highly correlated, a LASSO regression can be applied. By equation (25), we have that

$$\widetilde{\boldsymbol{\beta}}_i = \arg \min_{\boldsymbol{\beta}_i \in \mathbb{R}^p, (\boldsymbol{\beta}_i)_j = 0 (\forall j \in U^c)} \left\{ \frac{1}{2n} \left\| \mathbf{Y}_i - \widetilde{\mathbf{X}}_U(\boldsymbol{\beta}_i)_U \right\|_2^2 + \lambda \|\boldsymbol{\beta}_i\|_1 \right\} \quad (9)$$

where U^c denotes the complement of U . However, here we use a different λ as compared to the traditional LASSO. Normally the λ of LASSO is selected by cross-validation. However this will overfit the data as discussed in the paper [Zhu et al. \(2020\)](#). So here we use a modified version of the λ selection rule and set

$$\lambda = \max\{\lambda_{1se}, \min\{\lambda : \#supp(\widetilde{\boldsymbol{\beta}}_i) \leq 20\}\} \quad (10)$$

where $supp(\widetilde{\boldsymbol{\beta}}_i) = \{j : (\widetilde{\boldsymbol{\beta}}_i)_j \neq 0\}$. The notation $\#S$ means the number of elements in the set S . Here λ_{1se} is the λ selected by the “1se rule”. The “1se rule” gives the most regularized model such that error is within one standard error of the minimum

error achieved by the cross-validation (see [Friedman et al. \(2010\)](#); [Simon et al. \(2011\)](#); [Tibshirani et al. \(2012\)](#)). Therefore, we can derive the set of basis assets selected as

$$S_i \equiv \text{supp}(\tilde{\beta}_i) \quad (11)$$

Next, we fit an Ordinary Least-Square (OLS) regression on the selected basis assets, to estimate $\hat{\beta}_i$, the OLS estimator from

$$\mathbf{Y}_i = \alpha_i \mathbb{1}_n + \mathbf{X}_{S_i}(\beta_i)_{S_i} + \epsilon_i. \quad (12)$$

Note that $\text{supp}(\hat{\beta}_i) \subseteq S_i$. The adjusted R^2 is obtained from this estimation. Since we are in the OLS regime, significance tests can be performed on $\hat{\beta}_i$. This yields the significant set of coefficients

$$S_i^* \equiv \{j : P_{H_0}(|\beta_{i,j}| \geq |\hat{\beta}_{i,j}|) < 0.05\} \quad \text{where} \quad H_0 : \text{True value } \beta_{i,j} = 0. \quad (13)$$

Note that the significant basis asset set is a subset of the selected basis asset set. In another words,

$$S_i^* \subseteq \text{supp}(\hat{\beta}_i) \subseteq S_i \subseteq \{1, 2, \dots, p\}. \quad (14)$$

Then we look at the significant basis assets for the high- and the low-volatility portfolios separately by creating heatmaps. Each heatmap presents the percentage of selected factors in all of the ETF sectors.

A sketch of the GIBS algorithm is shown in [Table 1](#). Recall from the notation definition in [equation \(12\)](#) that for an index set $S \subseteq \{1, 2, \dots, p\}$, $\widetilde{\mathbf{X}}_S$ means the columns of the matrix $\widetilde{\mathbf{X}}$ indexed by the set S .

The Groupwise Interpretable Basis Selection (GIBS) algorithm
Inputs: Stocks to fit \mathbf{Y} and basis assets \mathbf{X} .
<ol style="list-style-type: none"> 1. Derive $\widetilde{\mathbf{X}}$ using \mathbf{X} and the Equation (7, 8). 2. Divide the transformed basis assets $\widetilde{\mathbf{X}}$ into k groups A_1, A_2, \dots, A_k using a financial interpretation. 3. Within each group, use prototype clustering to find prototypes $B_i \subset A_i$. 4. Let $B = \cup_{i=1}^k B_i$, use prototype clustering in B to find prototypes $U \subset B$. 5. For each stock \mathbf{Y}_i, use a modified version of LASSO to reduce $\widetilde{\mathbf{X}}_U$ to the selected basis assets $\widetilde{\mathbf{X}}_{S_i}$. 6. For each stock \mathbf{Y}_i, fit linear regression on \mathbf{X}_{S_i}.
Outputs: Selected factors S_i , significant factors S_i^* , and coefficients in step 6.

Table 1: The sketch of Groupwise Interpretable Basis Selection (GIBS) algorithm

We repeat this estimation process for all of the 3 year rolling regression windows ending with weeks in 2008 - 2018 (the time period we found in Section 2.2 with the low-volatility anomaly). Finally, we compare the significant basis assets selected for the high- and low-volatility portfolios. The results are given in the following Section 3.

3 Estimation Results

This section provides the results from our regressions employing both the FF5 and the AMF model.

3.1 Residual Analysis:

Can FF5 explain the low-volatility anomaly?

We first look at the time series plot of the cumulative capital from investing in the high- and low-volatility portfolios. Figure 3 in Section 2.2 shows the cumulative capital from the excess returns for both portfolios from 2008 to 2018. As evidenced in these graphs,

the two portfolios have different volatilities and the low-volatility portfolio outperforms the high-volatility portfolio.

Next, we calculate the cumulative capital from investing in the residual returns of the high- and the low-volatility portfolios. Figure 4 plots the FF5 model and Figure 5 plots the AMF model. Comparing Figures 3, 4, and 5, it is clear that the low-volatility anomaly is more pronounced in the excess returns as compared to the residuals. It is still obvious in the FF5 residuals, however, it almost disappears in the AMF residuals.

Formally, we can test for the differences between the cumulative capitals from these two portfolios. Since they have different volatilities, we use Welch's Two-sample t-test corrected for unequal variances. The hypotheses are

$$H_0 : \mu_l \leq \mu_h \quad H_A : \mu_l > \mu_h \quad (15)$$

where μ_l indicates the capital of the low-volatility portfolio, and the μ_h indicates the capital of the high-volatility portfolio. We do 3 tests where the cumulative capital is calculated with the excess returns, the residual returns from FF5, and the residual returns from AMF. If we reject the null-hypothesis H_0 , then there is strong evidence that the low-volatility anomaly exists.

The p-values of the tests are reported in the parentheses in Table 2. In the Table 2, the first row is the excess return, the second row is the FF5 residual return, and the third row is the AMF residual return. The first column gives the return to the low-volatility portfolios from 2008 - 2018. The second column is that of the high-volatility portfolios. The third column reports the difference between the two portfolios and gives the p-values of the tests in equation (15).

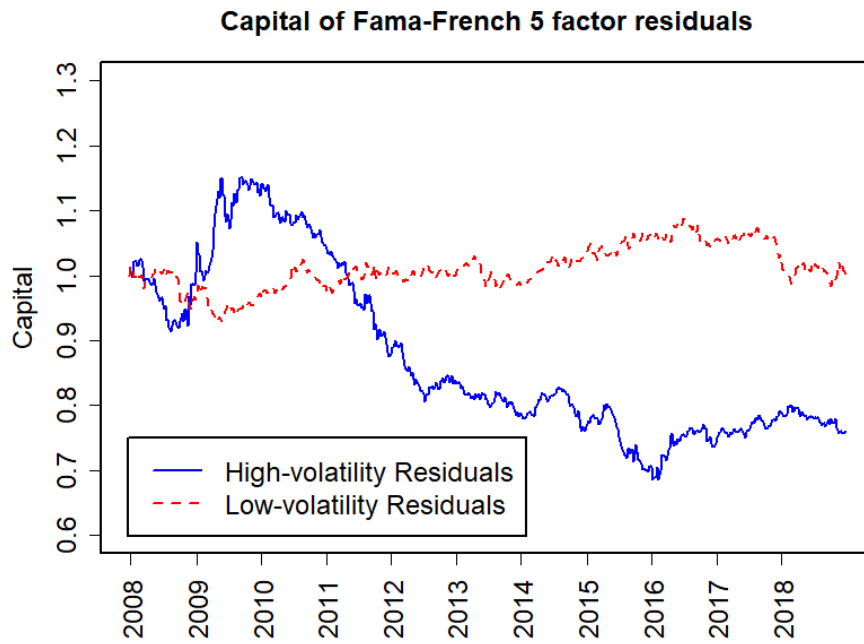


Figure 4: Cumulative capital plot of the FF5 residuals of the high-and low-volatility portfolios.

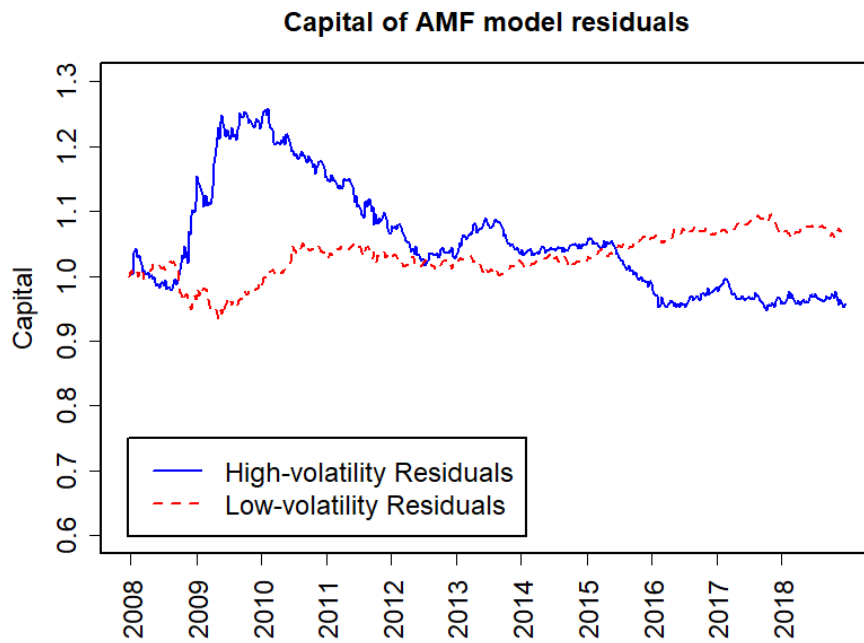


Figure 5: Cumulative capital plot of the AMF residuals of the high- and low-volatility portfolios.

	Low Portfolio	High Portfolio	Low - High (P value)
Excess return	1.21	0.62	0.59 (1.17×10^{-5})
FF5 residual return	-0.13	-0.31	0.18 (9.25×10^{-95})
AMF residual return	-0.05	-0.18	0.12 (1.00)

Table 2: Residual analysis comparing the FF5 and AMF models.

The p-value of the FF5 residual is still close to 0, rejecting the null hypothesis, thereby indicating that the low-volatility anomaly still exists after adjusting for risk using the FF5 model. In other words, the FF5 model cannot explain the low-volatility anomaly. However, the p-value of the AMF residual is close to 1, which implies that the low-volatility anomaly is not significant after adjusting for risk with the AMF model. Thus, the AMF model explains the low-volatility anomaly. Indeed, as we will see in Section 3.2 below, the AMF model shows that the two portfolios load on different basis assets (and implied risk factors). It is the (equilibrium) performance of these factors underlying the low-volatility portfolio that generates the low-volatility anomaly. Because the FF5 model makes the strong assumption that every security loads on the same 5 factors, it is not able to capture the low-volatility risk premium differences. This highlights the superior performance of the AMF model.

3.2 Factor Comparisons

In this section we compare the significant basis assets or “factors” selected by the GIBS algorithm for the two high- and low-volatility portfolios over 2008 - 2018. Figures 6 and 7 show the percentage of the significant factors for each ETF class selected by the GIBS algorithm for the low- and high-volatility portfolios each half-year across 2008 - 2018 (see Appendix D for more details on the ETF classifications).

As evidenced in the figures, the two portfolios load on very different factors. The low-volatility portfolio is mainly related to the ETFs in Bonds, Consumer Equities, and Real Estate. This is intuitive because bonds and real estate are of lower risk. Among the FF5 factors, the low-volatility portfolio only relates to the market return and the SMB factor. For the high-volatility portfolio, it mainly loads on ETFs in Materials & Precious metals, Consumer Equities, Health & Biotech Equities, and all the FF5 factors, except

Low-volatility portfolio significant factors

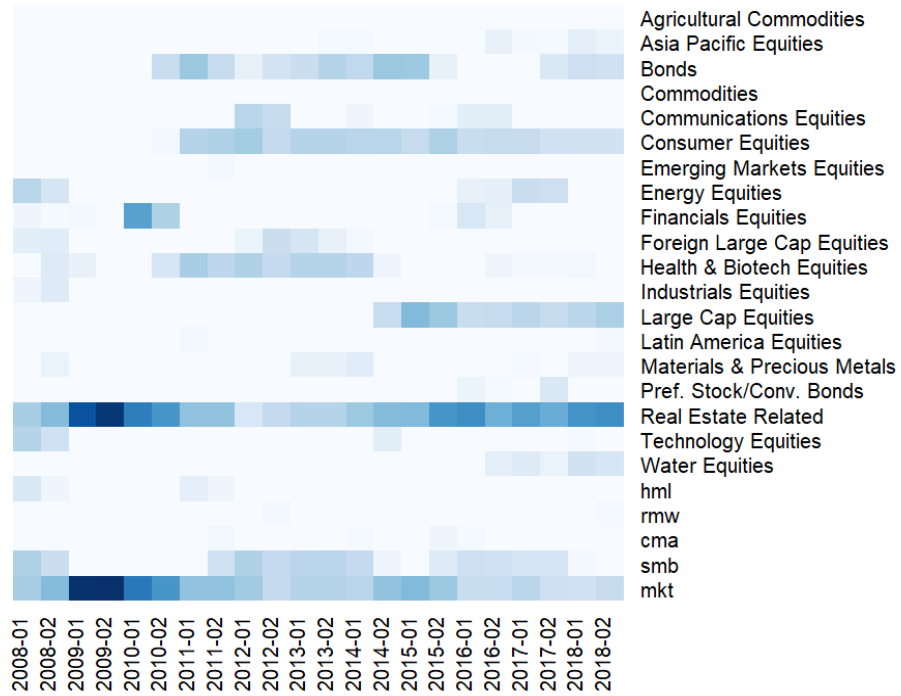


Figure 6: Heatmap for the low-volatility portfolio selected factors.

High-volatility portfolio significant factors

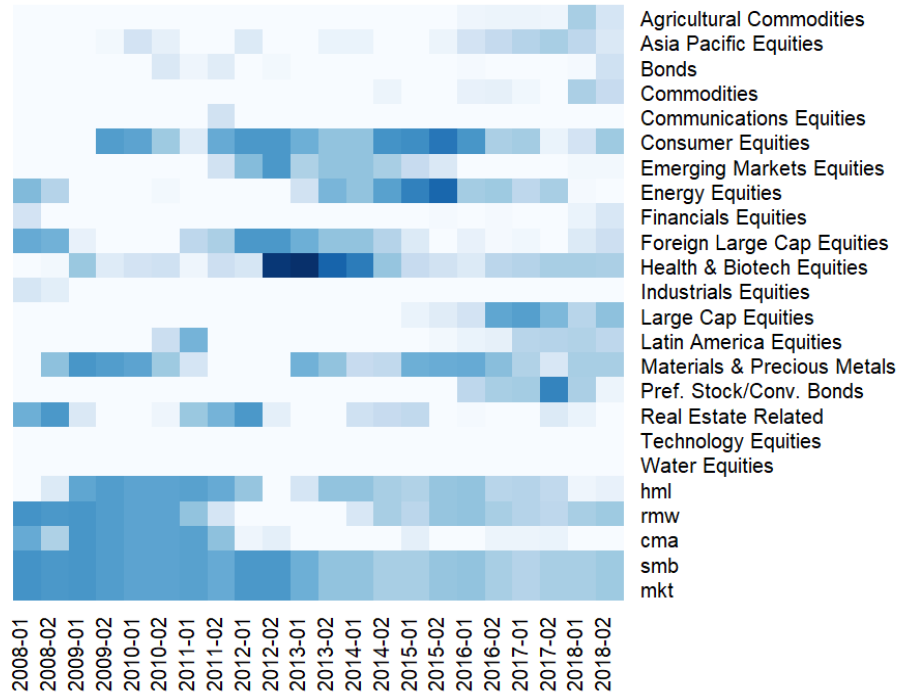


Figure 7: Heatmap for the high-volatility portfolio selected factors

CMA. The common factors for both portfolios are the market return, the SMB factor, and the Consumer Equity ETFs. Consequently, the out-performance of low-volatility portfolio is due to the different factor loadings, and reflects the differential performance of Bonds and Real Estate relative to materials, precious metals, and the healthcare industry.

Next, we provide a statistical test of whether the two volatility portfolios load on the same factors. Recalling the notation in equation (6), denote \mathbf{Y}_1 as the excess return to the low-volatility portfolio, and denote \mathbf{Y}_2 as the excess return to the high-volatility portfolio over the estimation period. From equation (11), denote S_1 and S_2 as the basis assets selected by GIBS for the low- and high-volatility portfolios, respectively. Then we let

$$\mathbf{Z} = \begin{pmatrix} \mathbf{Y}_1 \\ \mathbf{Y}_2 \end{pmatrix}_{2n \times 1}, \quad \mathbf{W} = \begin{pmatrix} \mathbf{X} \\ \mathbf{X} \end{pmatrix}_{2n \times 1}, \quad S = S_1 \cup S_2 \quad (16)$$

$$\mathbf{W}_S = \begin{pmatrix} \mathbf{X}_S \\ \mathbf{X}_S \end{pmatrix}_{2n \times 1}, \quad \mathbf{h} = \begin{pmatrix} \mathbf{0}_{n \times 1} \\ \mathbb{1}_{n \times 1} \end{pmatrix}_{2n \times 1} \quad (17)$$

The vector \mathbf{h} is an indicator vector which takes the value 1 for the high-volatility portfolio returns and 0 elsewhere.

The testing for the difference between the basis assets selected by the two volatility portfolios can be transformed to a testing for the significance of the interaction between \mathbf{h} and the selected factors \mathbf{W}_S . We fit two models

$$\text{Model 1: } \mathbf{Z} = \mathbf{W}_S \boldsymbol{\beta}_S + \boldsymbol{\epsilon} \quad (18)$$

$$\text{Model 2: } \mathbf{Z} = \mathbf{W}_S \boldsymbol{\beta}_S + [\mathbf{W}_S \odot (\mathbf{h} \mathbb{1}'_{2n})] \boldsymbol{\gamma}_S + \boldsymbol{\epsilon} \quad (19)$$

where \odot means the element-wise product for two matrices with the same dimension. Under the null hypothesis that the two portfolios have the same coefficients on the same factors, the goodness of fit of model 1 should be same as that of model 2. So we do an ANOVA(Model1, Model2) test to compare the two models. The results are in Table 3.

	Res.Df	RSS	Df difference	Sum of Sq	F statistic	Pr(>F)
Model 1	1139	0.24				
Model 2	1130	0.06	9	0.18	355.25	0.000

Table 3: The ANOVA test of the difference of the factors for the two portfolios.

The p-value of the test is approximately 0 to 3 decimal places, much smaller than 0.05, which means that the difference between model 1 and model 2 is significant. This is a strong evidence that the two volatility portfolios have different factor loadings, which validates the implications from the heatmap.

Another observation from the heatmaps is that the high-volatility portfolio is related to more basis assets than is the low-volatility portfolio. The number of basis assets selected by the GIBS algorithm and the number of significant basis assets among them is tabulated in Table 4 and graphed in Figures 8 and 9. We see that more basis assets are selected and significant for the high-volatility portfolio. This is intuitive because the larger volatility is generated by the uncorrelated risks of more basis assets in more volatile industries. More significant basis assets come from the ETF factors than from the FF5 factors. On average only 1.54 of the FF5 factors are significant for the low-volatility portfolio and 3.83 of the FF5 factors are significant for the high-volatility portfolio, manifesting a limitation of the FF5 model. Furthermore, most of the ETFs selected by the GIBS algorithm turn out to be significant, indicating that GIBS is more able to find relevant basis assets.

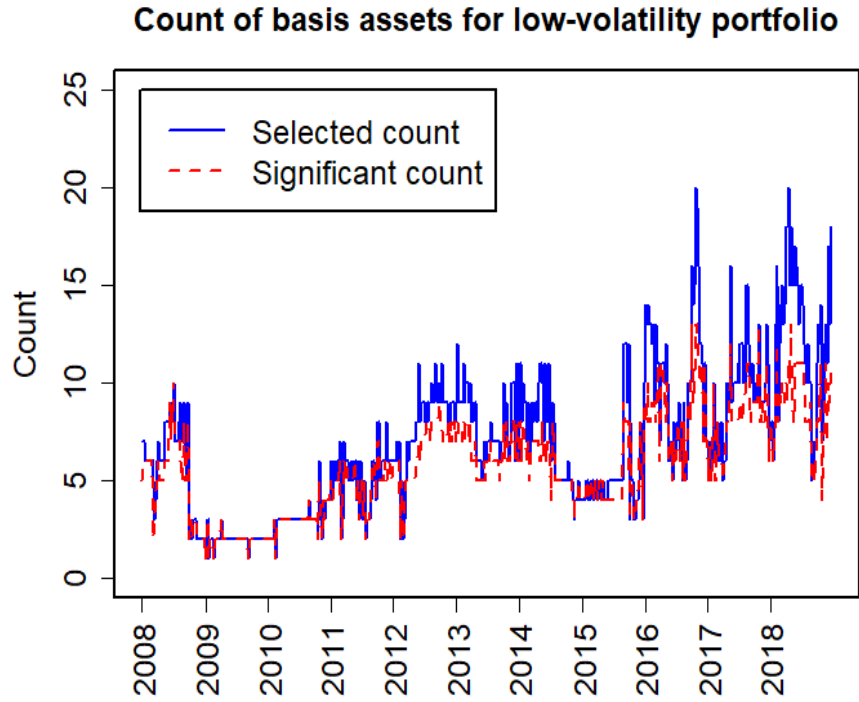


Figure 8: The number of selected and significant basis assets for the low-volatility portfolio.

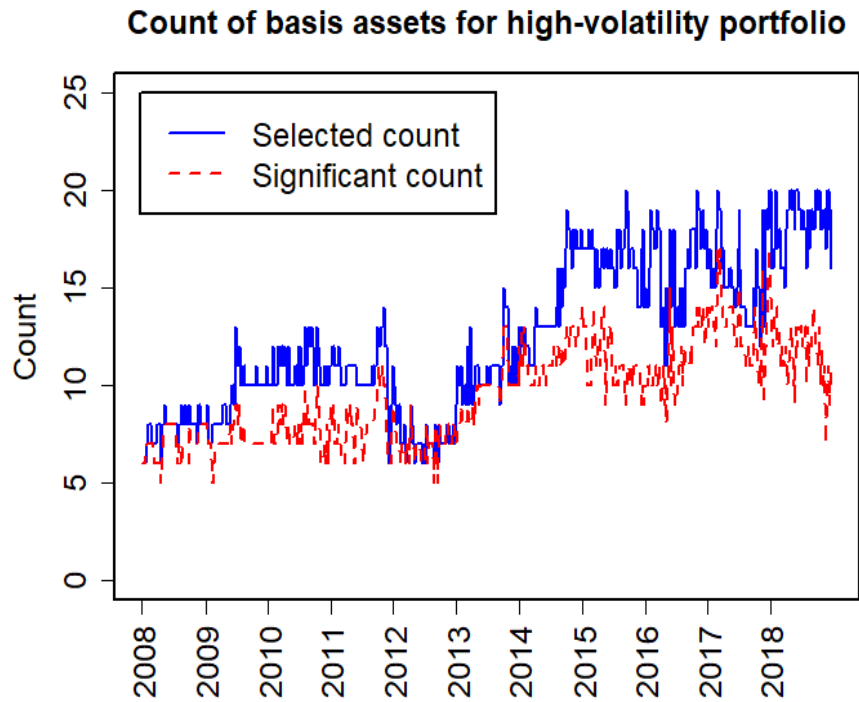


Figure 9: The number of the selected and significant basis assets for the high-volatility portfolio.

Portfolio	Select	FF5 Select	ETF Select	Signif.	FF5 Signif.	ETF Signif.
Low	6.96	1.72	5.23	5.82	1.54	4.29
High	12.50	4.12	8.38	9.53	3.83	5.70
Difference	5.54	2.39	3.15	3.71	2.29	1.41

Table 4: The number of the selected or significant basis assets / FF5 factors / ETFs for the two volatility portfolios. The “Select” column gives the mean number of basis assets selected by the GIBS algorithm. The “Signif.” column gives the mean number of significant basis assets among the selected ones. The number of the select / significant basis assets is the sum of the number of FF5 factors selected / significant and the ETFs selected / significant. The row “Low” is the results for the low-volatility portfolio, while the row “High” is for high-volatility portfolio. The row “Difference” gives the differences between two portfolios numbers using High - Low.

In summary, our estimation results show that the two volatility portfolios load on very different factors, which implies that volatility is not an independent risk measure, but that it is related to the identified basis assets (risk factors) in the relevant industries. It is the (equilibrium) performance of the loaded factors that results in the low-volatility anomaly and not disequilibrium (abnormal) returns.

3.3 Intercept Test

This section provides the tests for a non-zero intercept for both the AMF and FF5 pmodels for both volatility portfolios. This intercept test is a test for abnormal performance, i.e. performance inconsistent with the FF5 and AMF risk models. The null hypothesis is that the α 's in equation (2) are 0.

Figure 10 compares the distribution of the intercept test p-values for the FF5 and AMF models for the low-volatility portfolio, while Figure 11 is for the high-volatility portfolio. As we can see from the distribution plots, for both portfolios, the AMF model gives much larger p-values than does the FF5 model. Indeed, there are more weeks where a significant non-zero intercept is exhibited with the FF5 model as compared to the AMF model. This suggests that the AMF model is more consistent with market returns than is the FF5 model and that AMF model does a better job at pricing the anomaly. However, this difference could be due to the fact that we repeat this test 520 times (520 weeks in 2008 - 2018), and a percentage of the violations will occur and be observed even if the null

Portfolio	Percentage of Significant Weeks			
	FF5 $p < 0.05$	AMF $p < 0.05$	FF5 FDR $q < 0.05$	AMF FDR $q < 0.05$
High	30.1%	20.6%	0.00%	0.00%
Low	6.3%	2.6%	0.00%	0.00%

Table 5: Intercept Test with control of the False Discovery Rate. The first row is for the high-volatility portfolio, while the second row is for the low-volatility portfolio. The columns are related to p-values and False Discovery Rate (FDR) q-values for the FF5 model and the AMF model. For each column, we listed the percentage of weeks with significant non-zero intercept out of all the weeks in the 2008 - 2018 time period.

hypothesis is true. Hence, it is important to control for a False Discovery Rate (FDR).

We adjust for the false discovery rate using the Benjamini-Hochberg-Yekutieli (BHY) procedures [Benjamini and Yekutieli \(2001\)](#) since it accounts for any correlation between the intercept tests. Note that the Benjamini-Hochberg (BH) procedure [Benjamini and Hochberg \(1995\)](#) does not account for correlations, and in our case, weekly returns may be correlated. After adjusting for the false discover rate, for all weeks we fail to reject the non-zero hypothesis for both the FF5 and AMF models. The results are in Table 5. This evidence is consistent with the low- and high-volatility portfolios exhibiting no abnormal performance over our observation period.

3.4 In- and Out-of-Sample Goodness-of-fit Tests

This section compares both the In- and the Out-of-Sample Goodness-of-Fit tests for both the FF5 and the AMF model. For the In-Sample Goodness-of-Fit test, for each volatility portfolio, we record the adjusted R^2 's (see [Theil \(1961\)](#)) for both models for each rolling regression. Then, we calculate the mean of the adjusted R^2 's. The results are in the Table 6.

As shown in this table, even though the FF5 model does a good job in fitting the data, the AMF model is able to increase the adjusted R^2 's. We fit an ANOVA test comparing the FF5 model to the model using all the basis assets selected by GIBS and FF5. For all the rolling-window regressions over 2008 - 2018, the p-value of this ANOVA test is close to 0, less than 0.05. In another words, for all the weeks over 2008 - 2018, the AMF model has a significantly better fit than does the FF5 model, for both the low- and high-volatility

Distribution of intercept test p-values for the low portfolio

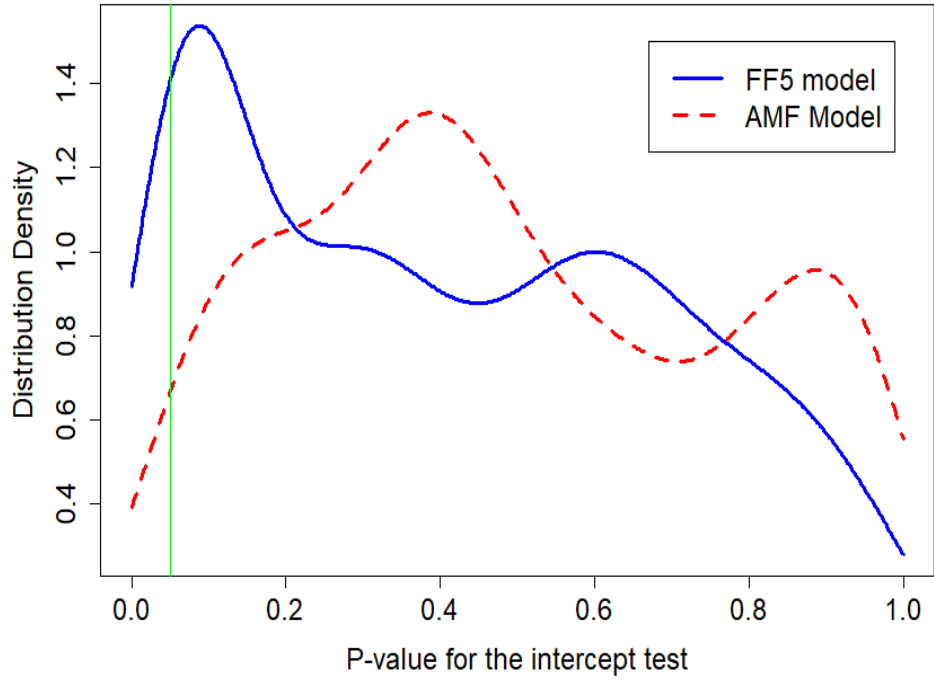


Figure 10: Distribution of intercept test p-values for the low-volatility portfolio.

Distribution of intercept test p-values for the high portfolio

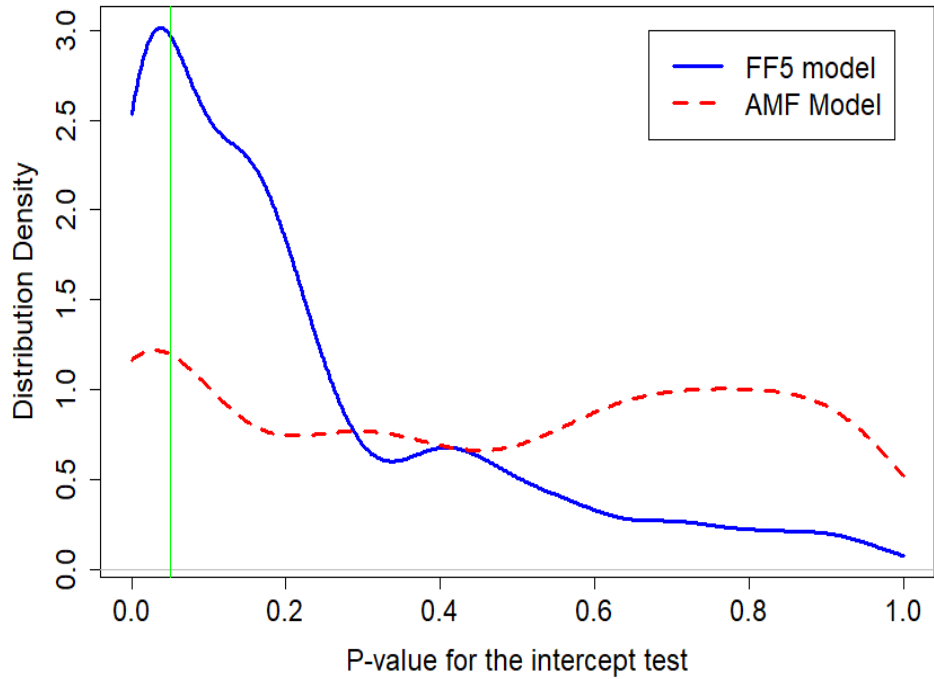


Figure 11: Distribution of intercept test p-values for the high-volatility portfolio.

Portfolio	FF5 Adj. R^2	AMF Adj. R^2 (change)	$p < 0.05$ Ratio	FDR $q < 0.05$ Ratio
Low	0.905	0.961 (+6.18%)	100%	100%
High	0.931	0.973 (+4.56%)	100%	100%

Table 6: In-Sample Goodness-of-Fit Tests.

Portfolio	FF5 Out-of-Sample R^2	AMF Out-of-Sample R^2 (change)
Low	0.951	0.973 (+2.25%)
High	0.973	0.982 (+1.01%)

Table 7: Out-of-Sample Goodness-of-Fit Tests.

portfolios. Since we do the tests 520 times (520 weeks in 2008 - 2018), we again need to adjust for the False Discovery Rate (FDR). However, even after adjusting the false discovery rate using the most strict BHY method accounting for the correlation between weeks, the FDR q -value is still smaller than 0.05 for all of the weeks. This is a strong evidence that the AMF out-performs the FF5.

For the Out-of-Sample Goodness-of-Fit test, we compare the 1-week ahead Out-of-Sample R^2 for the FF5 and AMF models for both volatility portfolios. The results are in Table 7. As it is seen in the table below, the AMF model out-performs the FF5 model in the prediction period, which indicates that the better performance of the AMF model is not due to over-fitting.

3.5 Risk Factor Determination

The AMF model selects the basis assets that best span a security's return. Some of these basis assets may not earn risk premium, and therefore, would not contribute to the risk premium earned by the volatility portfolios. This section studies which of the ETF basis assets correspond to risk-factors, i.e. factors that have non-zero expected excess returns.

At the end of our estimation period 2008 - 2018, there are 335 ETFs in the universe. Among them, the GIBS algorithm selects 35 ETF representatives in total. The list of these 35 ETF representatives is contained in Appendix C Table 10. Therefore, there are $35 + 5 = 40$ basis assets considering both the FF5 factors and ETFs together. In other words, $p_1 = 335$ and $p_2 = 40$ in Section 2.3. For each of these basis assets we compute

the sample mean excess return over our sample period. This is an estimate of the basis assets' risk premium.

The risk premium estimates for the Fama-French 5 factors are shown in Table 8. All of these are non-zero.

Fama-French 5 Factors	Market Return	SMB	HML	RMW	CMAF
Annual Excess Return (%)	13.2	-0.7	-1.7	0.9	-1.7

Table 8: Risk Premium of Fama-French 5 factors

The estimated risk premium for the ETFs are in Table 9. Out of the 35 ETF representatives selected by the GIBS algorithm, 23 of them have absolute risk premium larger than the minimum of that of the FF5 factors (which is the RMW with absolute risk premium 0.9%). This means that at least $(23 + 5)/(35 + 5) = 70\%$ basis assets are risk factors in the traditional sense. The list of the 23 ETFs that earns none-zero risk premium are listed in Table 9.

ETF name	Category	Risk Premium (%)
iShares MSCI Brazil ETF	Latin America Equities	44.0
VanEck Vectors Russia ETF	Emerging Markets Equities	20.6
iShares Mortgage Real Estate ETF	Real Estate	14.2
Invesco Water Resources ETF	Water Equities	13.9
Vanguard Financials ETF	Financials Equities	13.2
Vanguard FTSE Emerging Markets ETF	Emerging Markets Equities	12.3
VanEck Vectors Agribusiness ETF	Large Cap Blend Equities	12.3
Industrial Select Sector SPDR Fund	Industrials Equities	12.1
iShares Select Dividend ETF	Large Cap Value Equities	11.5
Materials Select Sector SPDR ETF	Materials	10.9
Vanguard Healthcare ETF	Health & Biotech Equities	10.2
iShares U.S. Home Construction ETF	Building & Construction	9.5
iShares MSCI Canada ETF	Foreign Large Cap Equities	9.4
SPDR Barclays Capital Convertible Bond ETF	Preferred Stock/Convertible Bonds	9.2
First Trust Amex Biotechnology Index	Health & Biotech Equities	8.1
Vanguard FTSE All-World ex-US ETF	Foreign Large Cap Equities	7.5
SPDR Barclays High Yield Bond ETF	High Yield Bonds	6.1
Invesco DB Agriculture Fund	Agricultural Commodities	-5.9
iShares MSCI Japan ETF	Japan Equities	5.8
iShares MSCI Malaysia ETF	Asia Pacific Equities	5.7
Invesco DB Commodity Index Tracking Fund	Commodities	4.9
iShares Gold Trust	Precious Metals	4.2
Vanguard Consumer Staples ETF	Consumer Staples Equities	3.8

Table 9: List of ETFs with large absolute risk premium.

4 Conclusion

In this paper we construct high- and low-volatility portfolios within the investable universe to explain the low-volatility anomaly using a new model, the Adaptive Multi-Factor (AMF) model estimated by the Groupwise Interpretable Basis Selection (GIBS) algorithm proposed in the paper by [Zhu et al. \(2020\)](#). For comparison with the literature, we compare the AMF model with the traditional Fama-French 5-factor (FF5) model. Our estimation shows the superior performance of the AMF model over FF5. Indeed, we show that the FF5 cannot explain the low-volatility anomaly while the AMF can. The AMF results show that the two volatility portfolios load on very different factors, which indicates that the volatility is not an independent measure of risk. It is the performance of the underlying risk factors that results in the low-volatility anomaly. Alternatively stated,

the out-performance of the low-volatility portfolio reflects the equilibrium compensation for the risk of its underlying risk factors.

References

- Ang, A., R. J. Hodrick, Y. Xing, and X. Zhang (2006). The cross-section of volatility and expected returns. *The Journal of Finance* 61(1), 259–299.
- Ang, A., R. J. Hodrick, Y. Xing, and X. Zhang (2009). High idiosyncratic volatility and low returns: International and further us evidence. *Journal of Financial Economics* 91(1), 1–23.
- Baker, M., B. Bradley, and J. Wurgler (2011). Benchmarks as limits to arbitrage: Understanding the low-volatility anomaly. *Financial Analysts Journal* 67(1), 40–54.
- Bali, T. G., S. J. Brown, S. Murray, and Y. Tang (2017). A lottery-demand-based explanation of the beta anomaly. *Journal of Financial and Quantitative Analysis* 52(6), 2369–2397.
- Benjamini, Y. and Y. Hochberg (1995). Controlling the false discovery rate: a practical and powerful approach to multiple testing. *Journal of the Royal Statistical Society: Series B (Methodological)* 57(1), 289–300.
- Benjamini, Y. and D. Yekutieli (2001). The control of the false discovery rate in multiple testing under dependency. *The Annals of Statistics* 29(4), 1165–1188.
- Bien, J. and R. Tibshirani (2011). Hierarchical clustering with prototypes via minimax linkage. *Journal of the American Statistical Association* 106(495), 1075–1084.
- Black, F. (1972). Capital market equilibrium with restricted borrowing. *The Journal of business* 45(3), 444–455.
- Black, F., M. C. Jensen, M. Scholes, et al. (1972). The capital asset pricing model: Some empirical tests. *Studies in the theory of capital markets* 81(3), 79–121.
- Fama, E. F. and K. R. French (2015). A five-factor asset pricing model. *Journal of Financial Economics* 116(1), 1–22.

- Feng, G., S. Giglio, and D. Xiu (2017). Taming the factor zoo. *Chicago Booth Research Paper* (17-04).
- Frazzini, A. and L. H. Pedersen (2014). Betting against beta. *Journal of Financial Economics* 111(1), 1–25.
- Friedman, J., T. Hastie, and R. Tibshirani (2010). Regularization paths for generalized linear models via coordinate descent. *Journal of Statistical Software* 33(1), 1.
- Giglio, S., Y. Liao, and D. Xiu (2020). Thousands of alpha tests. *Chicago Booth Research Paper* (18-09), 2018–16.
- Giglio, S. and D. Xiu (2019). Asset pricing with omitted factors. *Chicago Booth Research Paper* (16-21).
- Hong, H. and D. A. Sraer (2016). Speculative betas. *The Journal of Finance* 71(5), 2095–2144.
- Hsu, J. C., H. Kudoh, and T. Yamada (2013). When sell-side analysts meet high-volatility stocks: an alternative explanation for the low-volatility puzzle. *Journal of Investment Management* 11(2), 28–46.
- Jarrow, R. and P. Protter (2016). Positive alphas and a generalized multiple-factor asset pricing model. *Mathematics and Financial Economics* 10(1), 29–48.
- Kaufman, L. and P. J. Rousseeuw (2009). *Finding Groups in Data: An Introduction to Cluster Analysis*, Volume 344. John Wiley & Sons.
- Kozak, S., S. Nagel, and S. Santosh (2018). Interpreting factor models. *The Journal of Finance* 73(3), 1183–1223.
- McInish, T. H. and R. A. Wood (1986). Adjusting for beta bias: An assessment of alternate techniques: A note. *The Journal of Finance* 41(1), 277–286.
- Merton, R. C. (1973). An intertemporal capital asset pricing model. *Econometrica: Journal of the Econometric Society* 41(5), 867–887.

- Reid, S., J. Taylor, and R. Tibshirani (2018). A general framework for estimation and inference from clusters of features. *Journal of the American Statistical Association* 113(521), 280–293.
- Ross, S. A. (1976). The arbitrage theory of capital asset pricing. *Journal of Economic Theory* 13(3), 341–360.
- Shumway, T. (1997). The delisting bias in crsp data. *The Journal of Finance* 52(1), 327–340.
- Simon, N., J. Friedman, T. Hastie, and R. Tibshirani (2011). Regularization paths for cox’s proportional hazards model via coordinate descent. *Journal of Statistical Software* 39(5), 1.
- Theil, H. (1961). *Economic Forecasts and Policy*. North-Holland Pub. Co.
- Tibshirani, R. (1996). Regression shrinkage and selection via the lasso. *Journal of the Royal Statistical Society: Series B (Methodological)* 58(1), 267–288.
- Tibshirani, R., J. Bien, J. Friedman, T. Hastie, N. Simon, J. Taylor, and R. J. Tibshirani (2012). Strong rules for discarding predictors in lasso-type problems. *Journal of the Royal Statistical Society: Series B (Statistical Methodology)* 74(2), 245–266.
- Zhao, S., A. Shojaie, and D. Witten (2017). In defense of the indefensible: A very naive approach to high-dimensional inference. *arXiv preprint arXiv:1705.05543*.
- Zhu, L., S. Basu, R. A. Jarrow, and M. T. Wells (2020). High-dimensional estimation, basis assets, and the adaptive multi-factor model. *The Quarterly Journal of Finance* 10(04), 2050017.
- Zhu, L., R. A. Jarrow, and M. T. Wells (2021). Time-invariance coefficients tests with the adaptive multi-factor model. *arXiv preprint arXiv:2011.04171*.

Appendix A Low-risk anomaly review

The first explanation of the low-risk anomaly can be traced back to [Black et al. \(1972\)](#) who showed empirically using stock returns from 1926 to 1966 that expected excess returns on high-beta assets are lower than expected excess returns on low-beta stocks (with betas suggested by the CAPM). In a follow-up paper, accounting for borrowing constraints, [Black \(1972\)](#) proved that the slope of the line between expected returns and β must be smaller than when there are no borrowing restrictions. More recently, [Frazzini and Pedersen \(2014\)](#) document the low-beta anomaly in 20 international equity markets and across assets classes including Treasury bonds, corporate bonds, and futures. They argue that investors facing leverage and margin constraints increase the prices of high-beta assets, which generates lower alphas. They show that the Betting Against Beta (BAB) factor, which is long leveraged low-beta assets and short high beta assets, yields positive risk adjusted returns. [Ang et al. \(2006\)](#) find that stocks with high-idiosyncratic volatility after controlling for size, book-to-market, momentum, liquidity effects, and market-wide volatility risk (VIX) earn lower absolute and risk-adjusted returns than stocks with lower-idiosyncratic volatility. [Ang et al. \(2009\)](#) also show that there is a strong comovement in the anomaly across 27 developed markets which implies that easily diversifiable factors cannot explain the out performance of a low idiosyncratic volatility portfolio.

The behavioral explanations ([Baker et al. \(2011\)](#)) are that irrational investor preferences for lottery-like stocks (more attention is triggered if you talk about Tesla versus Procter & Gamble at a party) and an overconfidence bias pushes the prices of high risk stocks above their fundamentals. Second, because institutional investors have a mandate to outperform some market weighted index, they also over emphasize investments in high-risk stocks. By increasing the beta exposure of their portfolio in this way, they are more likely to beat the benchmark in a rising market. And, due to limits to arbitrage, “smart money” is not able to arbitrage away this low-risk anomaly. Providing additional support for this explanation, [Bali et al. \(2017\)](#) show that a proxy for lottery demand stocks (the average of the five highest daily returns in a given month) explains this low-beta anomaly. [Hong and Sraer \(2016\)](#) provide an equilibrium model consistent with this behavior. Last, it is also argued that the low-risk anomaly is tied to analyst earnings reports because high-risk stocks are characterized with more inflated sell side analyst’s

earnings growth forecasts which produce an investor overreaction and yields lower returns as shown in [Hsu et al. \(2013\)](#).

Appendix B Prototype Clustering and LASSO

This section describes the high-dimensional statistical methodologies used in the GIBS algorithm, including the prototype clustering and the LASSO. To remove unnecessary independent variables using clustering methods, we classify them into similar groups and then choose representatives from each group with small pairwise correlations. First, we define a distance metric to measure the similarity between points (in our case, the returns of the independent variables). Here, the distance metric is related to the correlation of the two points, i.e.

$$d(r_1, r_2) = 1 - |corr(r_1, r_2)| \quad (20)$$

where $r_i = (r_{i,t}, r_{i,t+1}, \dots, r_{i,T})'$ is the time series vector for independent variable $i = 1, 2$ and $corr(r_1, r_2)$ is their correlation. Second, the distance between two clusters needs to be defined. Once a cluster distance is defined, hierarchical clustering methods (see [Kaufman and Rousseeuw \(2009\)](#)) can be used to organize the data into trees.

In these trees, each leaf corresponds to one of the original data points. Agglomerative hierarchical clustering algorithms build trees in a bottom-up approach, initializing each cluster as a single point, then merging the two closest clusters at each successive stage. This merging is repeated until only one cluster remains. Traditionally, the distance between two clusters is defined as either a complete distance, single distance, average distance, or centroid distance. However, all of these approaches suffer from interpretation difficulties and inversions (which means parent nodes can sometimes have a lower distance than their children), see [Bien and Tibshirani \(2011\)](#). To avoid these difficulties, [Bien and Tibshirani \(2011\)](#) introduced hierarchical clustering with prototypes via a minimax linkage measure, defined as follows. For any point x and cluster C , let

$$d_{max}(x, C) = \max_{x' \in C} d(x, x') \quad (21)$$

be the distance to the farthest point in C from x . Define the *minimax radius* of the cluster

C as

$$r(C) = \min_{x \in C} d_{max}(x, C) \quad (22)$$

that is, this measures the distance from the farthest point $x \in C$ which is as close as possible to all the other elements in C . We call the minimizing point the *prototype* for C . Intuitively, it is the point at the center of this cluster. The *minimax linkage* between two clusters G and H is then defined as

$$d(G, H) = r(G \cup H). \quad (23)$$

Using this approach, we can easily find a good representative for each cluster, which is the prototype defined above. It is important to note that minimax linkage trees do not have inversions. Also, in our application as described below, to guarantee interpretable and tractability, using a single representative independent variable is better than using other approaches (for example, principal components analysis (PCA)) which employ linear combinations of the independent variables.

The LASSO method was introduced by [Tibshirani \(1996\)](#) for model selection when the number of independent variables (p) is larger than the number of sample observations (n). The method is based on the idea that instead of minimizing the squared loss to derive the Ordinary Least-Square (OLS) solution for a regression, we should add to the loss a penalty on the absolute value of the coefficients to minimize the absolute value of the non-zero coefficients selected. To illustrate the procedure, suppose that we have a linear model

$$\mathbf{y} = \mathbf{X}\boldsymbol{\beta} + \boldsymbol{\epsilon} \quad \text{where} \quad \boldsymbol{\epsilon} \sim N(0, \sigma_\epsilon^2 \mathbf{I}), \quad (24)$$

\mathbf{X} is an $n \times p$ matrix, \mathbf{y} and $\boldsymbol{\epsilon}$ are $n \times 1$ vectors, and $\boldsymbol{\beta}$ is a $p \times 1$ vector.

The LASSO estimator of $\boldsymbol{\beta}$ is given by

$$\hat{\boldsymbol{\beta}}_\lambda = \arg \min_{\boldsymbol{\beta} \in \mathbb{R}^p} \left\{ \frac{1}{2n} \|\mathbf{y} - \mathbf{X}\boldsymbol{\beta}\|_2^2 + \lambda \|\boldsymbol{\beta}\|_1 \right\} \quad (25)$$

where $\lambda > 0$ is the tuning parameter, which determines the magnitude of the penalty on the absolute value of non-zero β 's. In this paper, we use the R package *glmnet* [Friedman et al. \(2010\)](#) to fit LASSO.

In the subsequent estimation, we will only use a modified version of LASSO as a model selection method to find the collection of important independent variables. After the relevant basis assets are selected, we use a standard Ordinary Least-Square (OLS) regression on these variables to test for the goodness of fit and significance of the coefficients. More discussion of this approach can be found in Zhao, Shojaie, Witten (2017) [Zhao et al. \(2017\)](#).

In this paper, we fit the prototype clustering followed by a LASSO on the prototype basis assets selected. The theoretical justification for this approach can be found in [Reid et al. \(2018\)](#) and [Zhao et al. \(2017\)](#).

Appendix C Low-correlated ETF representative list

The low-correlated ETF name list in Section 3.5 is in Table 10.

ETF Names	Category
iShares Gold Trust	Precious Metals
iShares MSCI Malaysia ETF	Asia Pacific Equities
Vanguard FTSE All-World ex-US ETF	Foreign Large Cap Equities
iShares MSCI Canada ETF	Foreign Large Cap Equities
VanEck Vectors Agribusiness ETF	Large Cap Blend Equities
Vanguard FTSE Emerging Markets ETF	Emerging Markets Equities
VanEck Vectors Russia ETF	Emerging Markets Equities
PIMCO Enhanced Short Maturity Strategy Fund	Total Bond Market
iShares 3-7 Year Treasury Bond ETF	Government Bonds
SPDR Barclays 1-3 Month T-Bill ETF	Government Bonds
iShares Short Treasury Bond ETF	Government Bonds
iShares U.S. Home Construction ETF	Building & Construction
Alerian MLP ETF	MLPs
SPDR Barclays High Yield Bond ETF	High Yield Bonds
Vanguard Healthcare ETF	Health & Biotech Equities
SPDR Barclays Short Term Municipal Bond	National Munis
Materials Select Sector SPDR ETF	Materials

Continued on next page

ETF Names	Category
iShares MSCI Japan ETF	Japan Equities
WisdomTree Japan Hedged Equity Fund	Japan Equities
iShares Mortgage Real Estate ETF	Real Estate
Invesco DB Commodity Index Tracking Fund	Commodities
SPDR S&P Retail ETF	Consumer Discretionary Equities
Vanguard Financials ETF	Financials Equities
iShares MSCI Brazil ETF	Latin America Equities
iShares MSCI Mexico ETF	Latin America Equities
iShares Select Dividend ETF	Large Cap Value Equities
Invesco Water Resources ETF	Water Equities
SPDR DJ Wilshire Global Real Estate ETF	Global Real Estate
iShares North American Tech-Software ETF	Technology Equities
Consumer Staples Select Sector SPDR Fund	Consumer Staples Equities
SPDR Barclays Capital Convertible Bond ETF	Preferred Stock/Convertible Bonds
Invesco Preferred ETF	Preferred Stock/Convertible Bonds
Invesco DB Agriculture Fund	Agricultural Commodities
Industrial Select Sector SPDR Fund	Industrials Equities
SPDR FTSE International Government Inflation-Protected Bond ETF	Inflation-Protected Bonds

Table 10: Low-correlated ETF name list in Section 3.5.

Appendix D ETF Classes and Subclasses

ETFs can be divided into 10 classes, 73 subclasses (categories) in total, based on their financial explanations. The classify criteria are found from the ETFdb database: www.etfdb.com. The classes and subclasses are listed below:

1. **Bond/Fixed Income:** California Munis, Corporate Bonds, Emerging Markets

Bonds, Government Bonds, High Yield Bonds, Inflation-Protected Bonds, International Government Bonds, Money Market, Mortgage Backed Securities, National Munis, New York Munis, Preferred Stock/Convertible Bonds, Total Bond Market.

2. **Commodity:** Agricultural Commodities, Commodities, Metals, Oil & Gas, Precious Metals.
3. **Currency:** Currency.
4. **Diversified Portfolio:** Diversified Portfolio, Target Retirement Date.
5. **Equity:** All Cap Equities, Alternative Energy Equities, Asia Pacific Equities, Building & Construction, China Equities, Commodity Producers Equities, Communications Equities, Consumer Discretionary Equities, Consumer Staples Equities, Emerging Markets Equities, Energy Equities, Europe Equities, Financial Equities, Foreign Large Cap Equities, Foreign Small & Mid Cap Equities, Global Equities, Health & Biotech Equities, Industrials Equities, Japan Equities, Large Cap Blend Equities, Large Cap Growth Equities, Large Cap Value Equities, Latin America Equities, MLPs (Master Limited Partnerships), Materials, Mid Cap Blend Equities, Mid Cap Growth Equities, Mid Cap Value Equities, Small Cap Blend Equities, Small Cap Growth Equities, Small Cap Value Equities, Technology Equities, Transportation Equities, Utilities Equities, Volatility Hedged Equity, Water Equities.
6. **Alternative ETFs:** Hedge Fund, Long-Short.
7. **Inverse:** Inverse Bonds, Inverse Commodities, Inverse Equities, Inverse Volatility.
8. **Leveraged:** Leveraged Bonds, Leveraged Commodities, Leveraged Currency, Leveraged Equities, Leveraged Multi-Asset, Leveraged Real Estate, Leveraged Volatility.
9. **Real Estate:** Global Real Estate, Real Estate.
10. **Volatility:** Volatility.

In Section 3.2, we merged several categories to give a better visualization of the significant factors for each portfolio. The merged categories are

- Bonds: Corporate Bonds, Government Bonds, High Yield Bonds, Total Bond Market, Leveraged Bonds.
- Consumer Equities: Consumer Discretionary Equities, Consumer Staples Equities.
- Real Estate Related: Real Estate, Leveraged Real Estate, Global Real Estate, Utilities Equities,”Building & Construction.
- Energy Equities: Energy Equities, Alternative Energy Equities.
- Materials & Precious Metals: Materials, Precious Metals
- Large Cap Equities: Large Cap Blend Equities, Large Cap Growth Equities, Large Cap Value Equities.